Journal of Intelligent & Robotic Systems (2019) 94:621–637
https://doi.org/10.1007/s10846-018-0854-0

Admittance Controller with Spatial Modulation for Assisted Locomotion using a Smart Walker

Mario F. Jiménez[1] · **Matias Monllor**[2] · **Anselmo Frizera**[1] · **Teodiano Bastos**[1] · **Flavio Roberti**[2] · **Ricardo Carelli**[2]

Received: 16 November 2017 / Accepted: 17 April 2018 / Published online: 25 May 2018

Abstract

Smart Walkers are robotic devices that may be used to improve the stability in people with lower limb weakness or poor balance. Such devices may also offer support for cognitive disabilities and for people that cannot safely use conventional walkers. This paper presents an admittance controller that generates haptic signals to induce the tracking of a predetermined path. During use, when deviating from such path, the method proposed here varies the damping parameter of an admittance controller by means of a spatial modulation technique, resulting in a haptic feedback, which is perceived by the user as a difficult locomotion in wrong direction. The *UFES's Smart Walker* uses a multimodal cognitive interaction composed by a haptic feedback, and a visual interface with two LEDs to indicate the correct/desired direction when necessary. The controller was validated in two experiments. The first one consisted of following a predetermined path composed of straight segments. The second experiment consisted of finding a predetermined path starting from a position outside of such path. When haptic feedback was used, the kinematic estimation error was around 0.3 (± 0.13) m and the force applied to move the walker was approximately 5 kgf. When the multimodal interaction was performed with the haptic and visual interfaces, the kinematic estimation error decreased to 0.16 (± 0.03) m, and the force applied dropped to around 1 kgf, which can be seen as an important improvement on assisted locomotion.

Keywords Admittance control · Spatial modulation · Cognitive assistance · Haptic · Smart walker

1 Introduction

1.1 Motivation

The proportion of elderly people is growing in the world population. Between 2015 and 2030, the number of people aged over 60 years is projected to grow 56 percent, from 901 million to 1.4 billion. By 2050, the elderly population is projected to grow 56 percent more, reading nearly 2.1 billion individuals [1]. Older adults are the main community with physical and cognitive disabilities that affect the mobility [2]. Furthermore, independent locomotion may be affected by injuries, neurological diseases or surgical interventions. Diseases are the most common reason of locomotion impairment in people aged from 65 to 84 years old [3]. Stroke, Parkinson's disease, Alzheimer's dementia, degenerative joint disease, acquired musculoskeletal deformities, intermittent claudication, and impairments after an orthopedic surgery may also result in locomotion problems [2].

Mobilitiy assistive devices, such as canes, crutches, and conventional walkers can be used to increase the

✉ Mario F. Jiménez
mariof.jimenez@gmail.com; mario.hernandez@aluno.ufes.br

Matias Monllor
mmonllor@inaut.unsj.edu.ar

Anselmo Frizera
anselmo@ele.ufes.br

Teodiano Bastos
teodiano.bastos@ufes.br

Flavio Roberti
froberti@inaut.unsj.edu.ar

Ricardo Carelli
rcarelli@inaut.unsj.edu.ar

[1] Postgraduate Program in Electrical Engineering, Federal University of Espírito Santo, 29075-910 Vitoria, Brazil

[2] Institute of Automatics, National University of San Juan-CONICET, San Juan 5400, Argentina

user's base of support during gait to improve balance, and to promote safety and independence [4]. These devices improve the user's quality of life. When people have lower extremity weakness or poor balance, assistive devices such as conventional walkers improve stability, and facilitate mobility by increasing user's partial body weight support [5]. Walkers also decrease the risk of falling, with positive reflexes in the quality of life. However, conventional walkers can be difficult to maneuver [4] and, as a result, hard to navigate. Moreover, users may also require active support for guidance, orientation and location as they may suffer from cognitive disorders [6]. In these cases, more assistance can be required to promote independent locomotion than the one found on conventional walkers.

Technological advances have allowed the incorporation of actuators and sensors in walkers, providing assistance in gait for people with disabilities, which generally present problems in their motion and balance. Sensors can provide assistive navigation [7], localization [8], and obstacles detection and avoidance [9]. Also, they allow the identification of user's movement intention [10], which can be used in control strategies for mobility assistance, providing comfort, safety, and easy maneuverability of the walker [6]. These advanced walkers are termed *Smart Walker* (*SW*), which are able to provide physical support, sensorial assistance, cognitive assistance, health monitoring and advanced human–machine interface [6].

1.2 Human–Robot–Environment Interaction in Walker–Assisted Locomotion

There is a growing interest in developing robotic assistive devices for elderly, or people with physical and cognitive disabilities [11]. Similar to conventional walkers, *SWs* are used to provide mobility assistance to people with disabilities that present reduced lower motor function and low balance, by improving their autonomy, and, more generally, by improving their quality of life [12]. Through sensors, a *SW* may obtained information of the environment and detect the user's motion intention.

Research works have focused on *Human–Robot* interaction, which was usually supplied through sensors to detect the motion intention. In Guido [13], force sensors at the handlebar are used to detect the user intention. JAIST [14] and CAIROW [9] use a laser sensor to detect the user's leg position, and generate velocity control commands for the *SW*. In [10], the human movement intention is captured by force sensors on the arm support, and a LRF (Laser Range Finder) sensor that detects the legs' pose in relation to the walker. The user interacts in this case on a physical and cognitive level with the walker, as the *SW* follows the user velocity, and his/her motion intentions, resulting in a natural channel of communication. In [15], a controller for a human-robot formation is introduced, in which the human is the leader of the formation. LRF and ultrasound sensors are used to detect the user location and motion intentions. In this context, *SWs* can offer support for people with physical disabilities, and who cannot operate conventional walkers, reinforcing the personal autonomy and improving the daily living. However, when the user also presents cognitive impairments, it may be necessary to provide assistance at a different level. In this context, guidance and navigation functionalities may be an interesting approach to directly assist the user to reach the desired objective.

Despite the intense scientific and technological development around of the *SWs*, little attention has been paid to *Human–Robot–Environment* interaction. In [16], a shared control is proposed. The control architecture integrates cognitive, sensorial and physical assistance. A path following technique is used to support the cognitive assistance and, a LRF sensor is used for obstacle avoidance. CAIROW [9] has functions for path follower, localization and obstacle avoidance. All these *SWs* can guide people. However, none of them allow the user to make decisions about navigation.

In PAMM [17], an adaptive controller is implemented to guide the user back to a predetermined trajectory when the user deviates from it. It also detects its localization at the environment and, based on a performance evaluation, the controller generates a virtual force input based on the environment information to guide the user. The shared control included in PAMM allows that the user makes decisions about the *SW*, but, when the user deviates from the predetermined trajectory, the controller guides the user back to the trajectory. Although presented in some works, the authors understand that the use of supplementary forces, generated by the walker control strategy, must be avoided as external perturbations may compromise user's balance [17].

The *i-Walker* [8] promotes cognitive assistance, helping the user's guidance in common situations like moving uphill, downhill, turning left/right, and/or standing still, standing up, among others. Force sensors placed at the handlebars are used to detect the user's motion intention. Sensors installed on the environment helps navigation and promotes cognitive assistance. Nevertheless, the use of external sensors requires an extra investment to offer cognitive aid focused on memory reinforcements and activities of daily living support. Also, require known or predetermined environments to navigation. This could limit the user's independence.

In [7] and [18], the *SWs* provide sensorial assistance for blind people navigation. In those walkers, haptic feedback signals are provided through vibration of belt and the walker handles, to indicate the spatial information and navigation

commands. In both cases [7, 18], a laser sensor provides information for obstacle detection. The interpretation of the navigation commands requires a user's cognitive process. Such cognitive process introduce natural delays and may induce fatigue in the user [19].

Research works involve new sensors and control strategies to improve the *SWs* capabilities in different contexts [8, 10, 17, 20]. However, most of the *Human-Robot-Environment* interaction strategies found on the literature needs either wearable sensors and actuators on the individual, or sensors at the environment. Also, when the user is an elderly person and he/she is navigating with help from such devices, in some cases, a travel path can be programmed for an easy displacement, and the user does not make any decision about the *SW*, relieving the user from greater efforts and cognitive process. In this case, the user is just being guided by the*SW* and, has a secondary role in the *Human-Robot-Environment* interaction [7, 17, 21].

Therefore, it is necessary to develop a strategy with natural *Human–Robot–Environment* interaction, and thus, stimulate the cognitive system through decisions making, giving an active role to the user at navigation. Admittance control [16, 17] can be used to develop a natural interaction between the human and the *SW*, and also, to generate signals to indicate the path to follow in a real environment through a haptic feedback. The admittance control emulates a dynamic system and provides the user with a sensation of interaction with the *SW*. Through force sensors installed on the arm supports, motion intention can relate with linear and angular velocity [10, 22, 23].

In this work, a new proposal of controller that continuously modifies dynamic parameters of the admittance controller to induce the user to follow a predetermined path in a natural and intuitive way is presented. The proposed method generates a spatial modulation of the damping parameter, simulating a virtual canal for locomotion through variable friction, and inducing a sensation of hard navigation whenever the individual deviates from the right path or is outside of such virtual canal. The user perceives such sensation through the physical contact between his/her forearms and the SW structure. Furthermore, the user receives a haptic feedback as an increment in the difficulty of locomotion also when he/she is steering in the wrong direction.This way, the user needs to search the right direction and intuitively find the easy navigation. The proposed controller uses a multimodal cognitive interaction with the user through two channels. The first one is a haptic feedback that results from the physical interaction between user and SW. Interaction forces are acquired by means of tridimensional force sensors installed under the forearm supporting platforms. The second channel is a visual interface through two LEDs that indicate the direction that the *SW* should take to follow the right path. This way, the use of each channel does not get saturated. This control strategy induces the user to follow the path in a natural and intuitive way providing a "feeling" of command over the *SW*. Also, the user's cognitive system is stimulated through decision making when direction correction is needed.

Few works consider the variation of the admittance controller parameters for the user interacts with the environment. In [17], the author proposes a shared control with a cost function for the force signal, that combines the proximity to obstacles, the deviation from the planned trajectory and human stability criteria. The shared control varies force gains to provide more authority to the human or the robot. This way, the force signal of the admittance controller is variated. However, the user' motion intention may be affected because the user's force/torque signals do not command the smart walker. This change of robot control authority may produce a confusion sensation in the user and affects his/her cognitive system. With the control strategy presented in this work, it is affected the SW maneuverability on account of the damping parameter variation, but the user's motion intention is maintained. Nevertheless, the user needs to make decisions about of keep effort to drive the SW or correcting the locomotion direction and have an easier navigation. In [16], a shared control is proposed in order to on-line adapt the damping parameter of the admittance controller using the drift diffusion (DD) model proposed by [24]. That model describes the decision-making in humans as a process in which decisions are based on past decisions and the decision criteria are continuously adjusted in order to maximize the reward obtained throughout task execution[16]. Based on the DD model, decision maker blocks for sensorial, cognitive and physical assistance decide the level of robot assistance. As the user moves far away from the main task (desired path, obstacle avoidance), the controller assigns a higher decision making power to the robot, which makes the user lose maneuverability control on the robot. The strategy proposed in this work never takes away the user control of the robot. Furthermore, it allows varying in real-time the damping parameter of the admittance controller based on spatial information, and gives the user a main role in the *Human–Robot–Environment* interaction through a haptic sensation to discern the best path to follow.

This work is organized as follows. Section 2 describes the smart walker used and develops the *Human–Robot–Environment* interaction, describing how the admittance parameters are modulated. Section 3 describes the experimental setup, showing the way the user is guided along the path. Section 4 shows the experimental results, as well as the discussion about them. Finally, conclusions and future works are presented in Section 5.

2 Materials and Methods

The *SW* used in this work was developed at UFES/Brazil. Figure 1a shows the robotic platform and Fig. 1b shows the subsystems of the walker. The subsystems are described below.

Kinematic Structure The *SW* consists of a pair of differential rear wheels driven by DC motors, and a front caster wheel. The control commands for both motors are sent through power motor driver.

Odometry Wheels velocities are measured with optical shaft encoders H1 (US Digital, US). The robot orientation is determined through an 9 DOF inertial sensor BNO055. Both sensors are used to provide the robot's position and orientation in real-time.

CPU This subsystem is composed of an embedded computer (PC/104-Plus standard) for control and processing tasks. It consists of a 1.67 GHz Atom N450 with 2 GB of flash memory and 2 GB of RAM memory. This application is integrated into a real-time architecture based on Matlab-Simulink Real-Time xPC Target Toolbox. A computer is used to program the embedded computer and to store experimental data when necessary. It is connected to the PC/104-Plus by an ethernet interface using the UDP protocol.

Obstacle Detection A RP-LIDAR laser sensor is used as sensory assistant, retrieving information for obstacle detecting.

Interaction Sensors The *SW* has two 3D force sensors, model MTA400 (Futek, US), located under the forearm supporting platforms (Fig. 2). These sensors are used as a physical interface to determine the user's motion intentions (Fig. 2). The LRF sensor (Hokuyo URG-04LX) is the other interaction sensor that is used to obtain the distance between the user's legs and walker [10].The LRF sensor is employed for user safety, avoiding collisions between the user legs and the SW when the user motion intention is to drive the SW backwards.

2.1 Human–Robot–Environment Interaction (HREI)

A novel control strategy, shown in Fig. 3, is introduced here, which relies on admittance controller proposed in [16], to obtain the user's motion intention. The admittance controller emulates a dynamic system and gives the user a feeling as if he/she were interacting with the system specified by the admittance model [16]. A path following controller [25] is used to guide the user through a predetermined path. The objective of the path following controller is to provide a desired orientation to the *SW*. The admittance modulator takes the orientation error and the user's torque intention to change, in real-time, damping parameters of the admittance controller. A supervisor is used to establish safe parameters for the user. Each block in Fig. 3 is explained in the following sections.

The user's motion intention is determined through force sensors located under the forearm supporting platforms (see Fig. 2). The signals from the *y* axes of each sensor are used

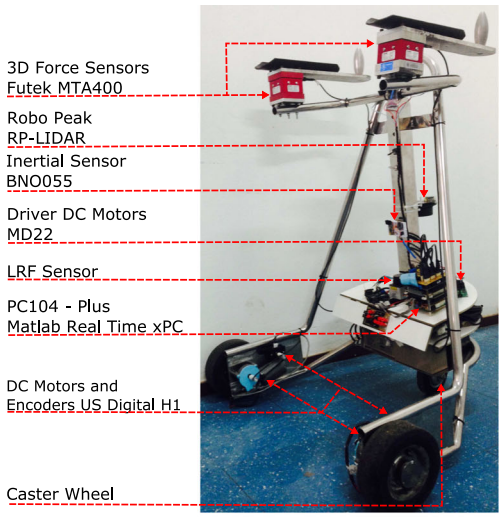

(a)

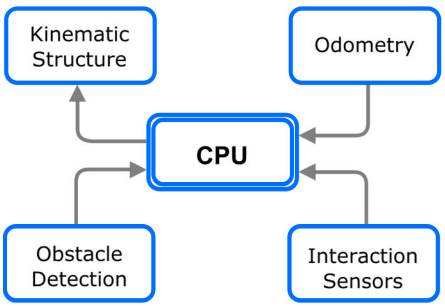

(b)

Fig. 1 **a** Smart Walker of UFES/Brazil; **b** Subsystems inside the walker

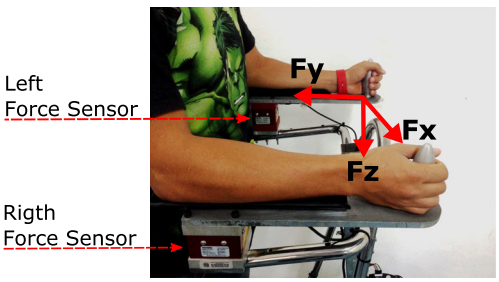

Fig. 2 *Human–Robot* interaction system based on force sensors

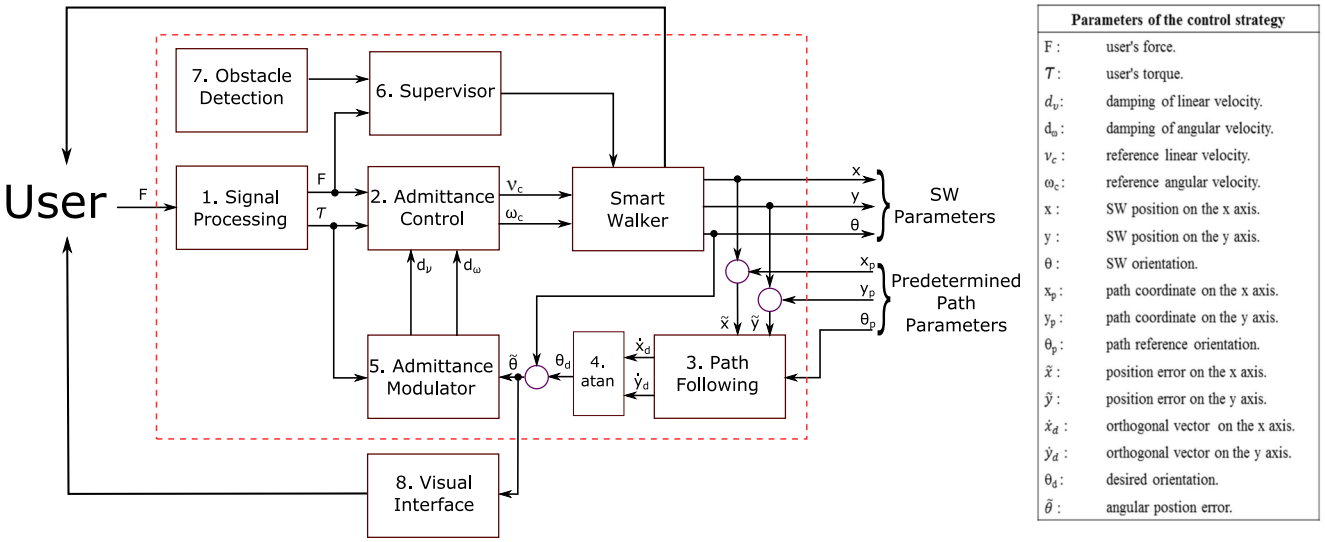

Parameters of the control strategy	
F :	user's force.
T :	user's torque.
d_v :	damping of linear velocity.
d_ω :	damping of angular velocity.
v_c :	reference linear velocity.
ω_c :	reference angular velocity.
x :	SW position on the x axis.
y :	SW position on the y axis.
θ :	SW orientation.
x_p :	path coordinate on the x axis.
y_p :	path coordinate on the y axis.
θ_p :	path reference orientation.
$\tilde{x}$:	position error on the x axis.
$\tilde{y}$:	position error on the y axis.
$\dot{x}_d$:	orthogonal vector on the x axis.
$\dot{y}_d$:	orthogonal vector on the y axis.
θ_d :	desired orientation.
$\tilde{\theta}$:	angular postion error.

Fig. 3 Block diagram of the controller with admittance modulation

to obtain force and torque measurements (box 1 Fig. 3), depending on the arm motion, as shown in Eqs. 1 and 2.

$$F(t) = \frac{-(F_{L_Y}(t) + F_{R_Y}(t))}{2} \tag{1}$$

$$\tau(t) = \frac{-(F_{L_Y}(t) - F_{R_Y}(t))}{2}.d, \tag{2}$$

where F_{L_Y} is the force on the left arm, F_{R_Y} is the force on the right arm, and d is the distance between sensors. F and τ can be computed to obtain the desired reference velocity for the *SW* [16]. The linear control velocity $v_c(t)$ and angular control velocity $\omega_c(t)$, (box 2 Fig. 3) are calculated as shown in Eqs. 3 and 4 respectively.

$$v_c(t) = \frac{F(t) - m_v\dot{v}(t)}{d_v(t)} \tag{3}$$

$$\omega_c(t) = \frac{\tau(t) - m_\omega\dot{\omega}(t)}{d_\omega(t)} \tag{4}$$

The masses m_v and m_ω, and damping d_v, d_ω are parameters of the admittance control that shape the interaction dynamics *Human–Robot–Environment*.

To guide the user through a predetermined path, a path following controller is used (box 3 Fig. 3), which uses the kinematic model of an unicycle-like mobile robot [26]. The use of the kinematic model for controlling the movement of the *SW* is based on the fact that the assistance device moves with slow velocities and accelerations. In that sense, it is not necessary to apply a dynamic model, because the dynamic imposed by the admittance control is slow when compared with the robot dynamics.

As the user has the domain of the walker, the path following controller provides the reference orientation. Such desired orientation is calculated through the control structure for path following developed by Andaluz et al. [25]. The reference point is placed in the middle of rear wheels axis, at the initial user's feet position. In closed loop, the equation is defined in the following way:

$$\begin{bmatrix} \dot{x}_d \\ \dot{y}_d \end{bmatrix} = v_p + v_a, \tag{5}$$

where v_p is the path velocity vector and v_a is the path attraction velocity vector. Hence, the full equation is represented by:

$$\begin{bmatrix} \dot{x}_d \\ \dot{y}_d \end{bmatrix} = \begin{bmatrix} v_r cos\theta_p + l_x tanh\left(\frac{k_x}{l_x}\tilde{x}\right) \\ v_r sin\theta_p + l_y tanh\left(\frac{k_y}{l_y}\tilde{y}\right) \end{bmatrix}, \tag{6}$$

where v_r is the path desired velocity; θ_p is the path reference orientation, defined by the tangent of the nearest point to the path; l_x and l_y establish the saturation limits of position error; k_x and k_y are constant gains that determine the slope of the $tanh$; $\tilde{x}$ and $\tilde{y}$ are the position errors of the robot with respect to the path; v_{SW} is the *SW* velocity (see Fig. 4). The function in closed loop (6) is used to calculate the desired orientation θ_d (box 4 Fig. 3) shown in Eq. 7 (see Fig. 4), which is generated from the orthogonal vectors $\dot{x}_d$ and $\dot{y}_d$, and is the strategy proposed to relate the path following controller with the *HREI*.

$$\theta_d = atan\left(\frac{\dot{y}_d}{\dot{x}_d}\right) \tag{7}$$

2.1.1 Admittance Spatial Modulator

The key difference from the controller used here compared to the classical admittance controller, is that it allows the variation of its dynamic parameters according to sensors input signals. The admittance modulator (box 5 Fig. 3) is

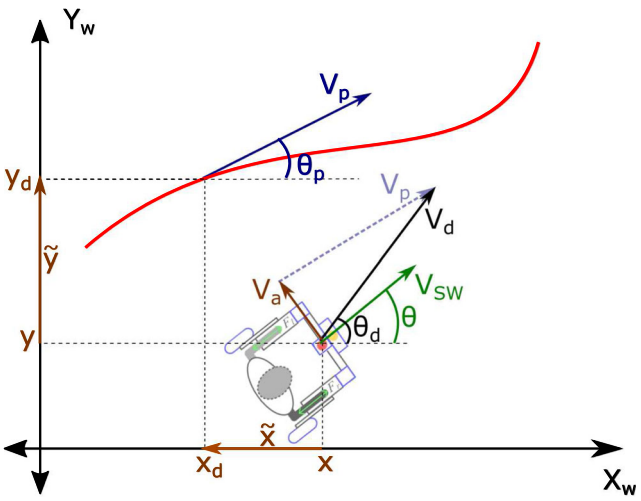

Fig. 4 Predetermined path for following

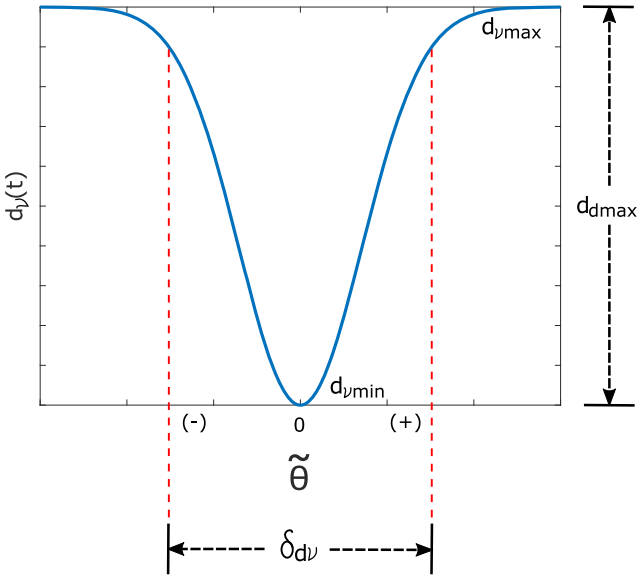

Fig. 6 Curve of damping force d_v

in charge to generate the signals that produce the haptic sensation of the control strategy here proposed.

The new strategy of the *admittance spatial modulator* is used to change the damping parameter of Eqs. 3 and 4, as a function of information collected from the environment. The damping d_v and d_ω are the dynamic parameters of the admittance control which allows the desired *HWEI*, and can increase or decrease the linear velocity $v_c(t)$ and angular velocity $\omega_c(t)$.

The admittance modulator is in charge of establishing a dynamic signal that modifies the damping parameter in the admittance controller, thus generating the haptic feedback. This modulator has as input variables the desired orientation θ_d and the *SW* orientation θ (see Fig. 5). The angular position error ($\tilde{\theta}$), shown in Eq. 8, is calculated with respect to the actual orientation θ of the *SW*. Such errors occur when the robot has diverted from its path.

$$\tilde{\theta} = \theta_d - \theta \tag{8}$$

Now, it is necessary to establish the curves that modify in real-time the parameters of the admittance control, and, in this way, guide the user by the predetermined path. The damping parameter implicitly hints the correct direction of the path following, decreasing when the device is on the correct path.

From Eq. 3, the parameter m_v remains constant, and d_v has an inverted gauss behavior (see Fig. 6), because this function offers changes with soft transitions, which are

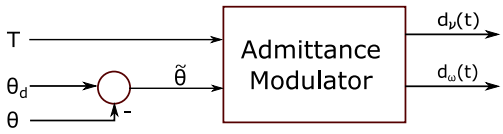

Fig. 5 Block diagram of the admittance modulator

reflected in the user experience.The function describing the curve in Fig. 6 is shown in Eq. 9.

$$d_v(t) = d_{vmax} - d_{dmax} e^{\left(-\frac{\tilde{\theta}}{\delta_{dv}}\right)^2}, \tag{9}$$

where, d_{vmax} is the maximum limit of $d_v(t)$; d_{dmax} is the maximum decrease of velocity damping (see Eq. 3); and δ_{dv} is the parameter that determines the width of $d_v(t)$ function. (see Eq. 3).

This way, when $\tilde{\theta}$ is zero, the damping is minimum allowing the *SW* to move with great facility. The bigger the orientation error, the bigger will be the locomotion difficulty with the *SW*. Also, the linear velocity $v_c(t)$ decreases.

To define d_v, it is necessary to take into account (see Fig. 6):

d_{vmax}: maximum damping wished for linear velocity (see Eq. 3)
d_{dmax}: maximum variation of $d_v(t)$ function. ($d_{vmax} - d_{vmin}$).
δ_{dv}: $\tilde{\theta}$ for maximum damping.

For ω_c, the same restriction as in v_c is taken, i.e., m_ω remains constant. In Eq. 4, the definition of d_ω is given by:

$$d_\omega(t) = d_{i\omega} + G_{d\omega} tanh\left(\frac{1}{P_{d\omega}} \tau\tilde{\theta}\right), \tag{10}$$

where $d_{i\omega}$ is the initial damping value in the angular velocity $\omega_c(t)$; $G_{d\omega}$ is the gain variation of the torque damping (see Eq. 4), and $P_{d\omega}$ is the variation slope of curve of d_ω.

It is necessary to take into account the following restriction in Eq. 10,

$$d_{i\omega} > G_{d\omega}$$

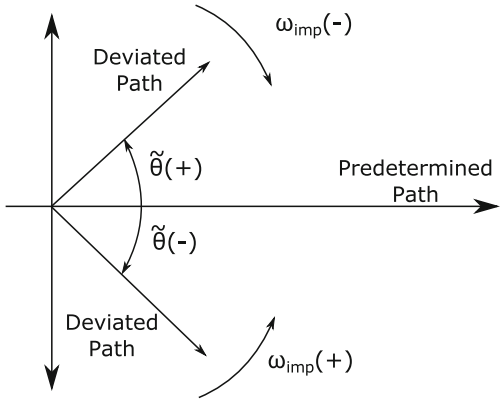

Fig. 7 Criterion for orientation correction

to avoid having negative values in $d_\omega(t)$. When $\tilde{\theta}$ is positive and the user's torque τ induces a negative ω_c, and vice versa, it implies that the walker's user intents to correct the angular position error (see Fig. 7). In this context, when $\tilde{\theta}$ becomes smaller d_ω tends to decrease. On the contrary, the user has to apply more effort to turn the *SW*.

To define d_ω, it is necessary to take into account (see Fig. 8):

$d_{i\omega}$: (maximum damping desired($d_\omega max$) + minimum damping desired($d_\omega min$))/2.
$G_{d\omega}$: (maximum damping desired($d_\omega max$) - minimum damping desired($d_\omega min$))/2.
$P_{d\omega}$: defined by empirical criterion in function of haptic feedback.

The spatial modulation of d_v and d_ω can be adjusted on the limits where the user starts to feel the haptic feedback (i.e. mobility difficulty when the walker does not follow a predetermined path). The user interprets the *SW* movement within the limits as a virtual mobility canal that allows easier locomotion. Furthermore, the cognitive interface provided by the haptic feedback interacts with the user through a process of decision-making about the path to follow, keeping the brain active.

2.1.2 Safety Supervisor

Although the *SW* offers a stable assistance for walking, when working with an active robotic helper [21], it is necessary to establish safety parameters for the user through a sensory assistant and a cognitive interface, in order to have a safe *HWEI*. In this case, a supervisor (box 6 Fig. 3) with three safety factors was implemented . The first safety rule regards the user's partial body weight support on the *SW* platform, which has a threshold of 0.6 kgf in the z axis of each force sensor. If a threshold is not surpassed, no motor/control command is sent to the drivers. In this manner, a suitable posture or body weight support is necessary for the system to operate. Otherwise, the robot remains blocked to allow the user to position himself/herself. Once the controller detects that the threshold was reached in each sensor, v_c and ω_c assume the values defined by the control strategy. In the second safety rule, a protection zone with 70 cm of radio around the RP-LIDAR laser sensor is defined (see Fig. 9), therefore, if the laser sensor detects an obstacle within the interest zone (box 7 Fig. 3), v_c and ω_c become zero to avoid a possible collision, if the contrary happens, they acquire the values of velocity provided by the controller. As obstacle avoidance is not the object of this study, this simple solution was implemented to guarantee user's safety when navigating with the robotic device. Another safety rule defines a lower limit of 20 cm and an upper limit of 50 cm of distance between the user and the SW. This way, when the user drives the SW backwards and the LRF sensor measures a distance smaller than the established lower limit, v_c and

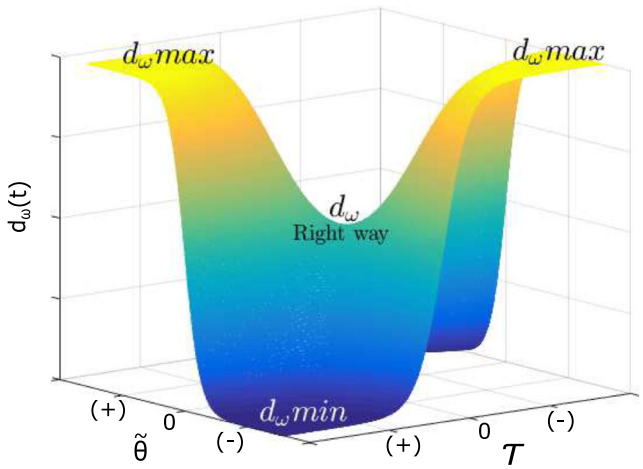

Fig. 8 Curve of torque damping d_ω

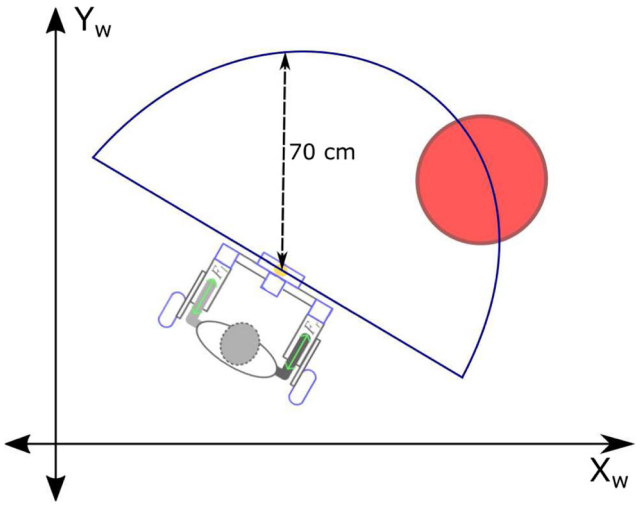

Fig. 9 Obstacle detecting zone

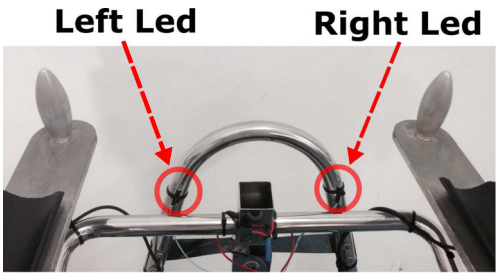

Fig. 10 Position of LEDs on the *UFES SW*

ω_c become zero to avoid collisions between the user's legs and the *SW*. Furthermore, when the LRF sensor measures a distance higher than the upper limit, v_c and ω_c also become zero to avoid user falls. Otherwise, the SW is driven by the velocities obtained from the proposed controller.

2.1.3 Visual Interface

Two LEDs are used as visual interface with the user (Fig. 10). Such visual interface (box 8 Fig. 3) indicates to the user the correct orientation when the walker is outside the predetermined path. As the controller establishes a virtual mobility canal for easier locomotion, a limit of $\pm\ 25^0$ for $\tilde{\theta}$ was defined, because, before this limit, d_v takes a value that allows an easier maneuverability with the *SW*. Also, the limit in $\tilde{\theta}$ allows that the visual channel of the multimodal cognitive interface does not saturate the user's vision. Once $\tilde{\theta}$ surpasses the error limit, the LEDs indicate the turn intention that the user should make, and, this way correcting the error in $\tilde{\theta}$. The LEDs lights on according to the turn recommendation. When the user achieves the correct direction, the two LEDs power off. The visual interface assists cognitively the user to achieve the correct direction to come back to the predetermined path, complementing the haptic feedback.

3 Experimental Setup

Eight people (28.5±5.42 years old) and without without any history of gait dysfunctions and with no previous training with the *SW* participated of the experiments. The purpose of this work is to show the initial validation of the control strategy. For this reason, the validation with patients (elderly people with mobility and cognitive impairments) will be the focus of future research. A computer was used to program the embedded computer (PC/104-Plus) and to record the experiment data. The data recorded were: control signals (ω_c, v_c, d_v, d_ω, $\tilde{\theta}$), SW position (x, y), linear and angular velocities and LEDs signals; in addition to user-walker interaction parameters (F and τ) and user legs distance to SW (using LRF sensor). The control strategy was programmed in Matlab-Simulink Real-Time xPC Target Toolbox, and downloaded to the PC/104-Plus. Two different paths unknown by the participants were proposed, which were used to evaluate the controller performance and the cognitive interaction. In order to improve the *HREI*, the user weight was taken into account. It was found an empirical relation between the user weight and the values to be assigned to the constants m_v and m_ω in Eqs. 3 and 4 respectively. The weight range of participants was 53.6 kg to 101.6 kg (see Table 1). Once the constants of virtual mass were known, it was verified that the user could move the *SW* comfortably through a short path in straight line. The other constants values used in the controller were determined empirically from the experiments with the control strategy, which are described in Table 2.

Table 1 Virtual mass values and user weight

User No.	Weight [kg]	m_v [kg]	m_ω [kg]
1.	53.6	1.8	1.3
2.	57.4	1.3	1
3.	58	1.3	1
4.	60.4	1.8	1.4
5.	61.4	2	1.5
6.	65.4	3.8	3.5
7.	71.7	3.3	3
8.	101.6	3.8	3.5

Table 2 Constants values used in the control strategy

Path following	
Constant	Value
k_x	0.7
k_y	0.7
l_x	3
l_y	3
v_r	0.3
Spatial modulator of d_v	
Constant	Value
$d_{v_{max}}$	30
$d_{d_{max}}$	29.5
δ_{d_v}	0.8
m_v	see Table 1
Spatial modulator of d_ω	
Constant	Value
d_{i_ω}	4
G_{d_ω}	3.5
P_{d_ω}	2
m_ω	see Table 1

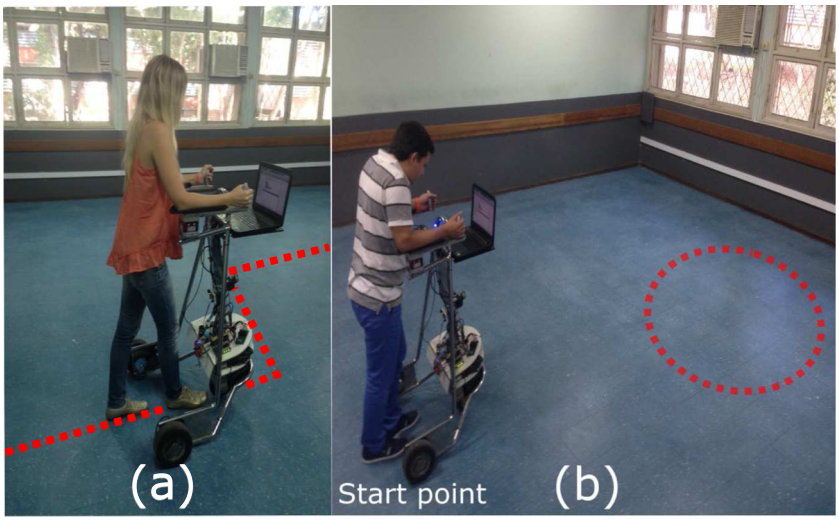

Fig. 11 Experiments with different paths. **a** Experiment No. 1 (Following straight segments). **b** Experiment No. 2 (Finding the circle path)

3.1 Experiment No.1. Following Straight Segments

The intention of the first experiment was to observe the controller behavior using the multimodal cognitive interface and the haptic feedback. Here, the user voluntarily went outside of the predetermined path. The start point of the experiment was at x = 0 and y = 0. A path made of three segments linked with angles of 90^o was used (see Fig. 11a). This path has a first segment of 2.6 m in a straight line, then a left turn of 90^o, followed of a straight segment of 1.5 m, and at last, a right turn of 90^o for a final segment of 10.4 m in a straight line. The points of the path were set every 0.2 m. On the first part of the experiment, the user was asked to be guided by the LED indications of the *SW* until reaching the end point, which was 5.2 m. On the second part, in one of the turns, the user was asked to ignore the controller recommendations and try to maintain in the straight direction, in such a way that the user could feel the controller action through the haptic feedback. When the *SW* became difficult to maneuver, the user was asked to follow the visual interface by LEDs and re-direct the walker in the right direction.

3.2 Experiment No.2. Finding the Circle Path

The second experiment was conducted to validate the path following controller, and to observe the controller guiding action when the user was outside of the path. In this experiment, as a hypothetical case, the user starts the locomotion outside the predetermined path (see Fig. 11b). A circle was used as predetermined path, with radio of 2 m, and center at $x = 3$ and $y = 0$. The start point of the experiment was at $x = 0$ and $y = 0$. At this experiment, the user had greater interaction with the haptic feedback when is compared to the experiment No. 1. In this case, the user had to feel the changes of locomotion difficulty of the *SW* to find the path. In the first experiment, the user had to find the circle path using a haptic feedback only. In the second experiment, the user had to use the multimodal cognitive interface to find the circle path.

3.3 Experiment No.3: Supervisor Functionality

The third experiment was conducted to verify the supervisor functionality. A straight line path of 15 m was used, and it was checked that the linear and angular velocities became zero when the *SW* was very close to obstacles, or when the threshold in the z axis for the two sensors was not exceeded. The obstacles were located at coordinates (6, 0) and (9, 0). The bad user's posture was simulated at the beginning and the end of the predetermined path in this experiment.

4 Results and Discussion

4.1 Experiment No.1: Following the Straight Path

In the first experiment, users were asked to follow a predetermined path while complying with recommendations from the multimodal cognitive interaction. Figure 12a shows the results from one participant for the first part of the experiment. It can be seen that the LEDs indications were useful to hint the predetermined path, allowing the user to stay on the path most of the time.

A representative result of the second part of the experiment No. 1 is shown in Fig. 12b. In this case, the data collected from user 7 (see Table 1) was used. In such case, the user was asked to go ahead at the straight path and to ignore the turn recommendation given by the visual cognitive interface. By doing so, when deviating from the predetermined path, the user felt the haptic feedback provided by the controller. As a consequence, physical

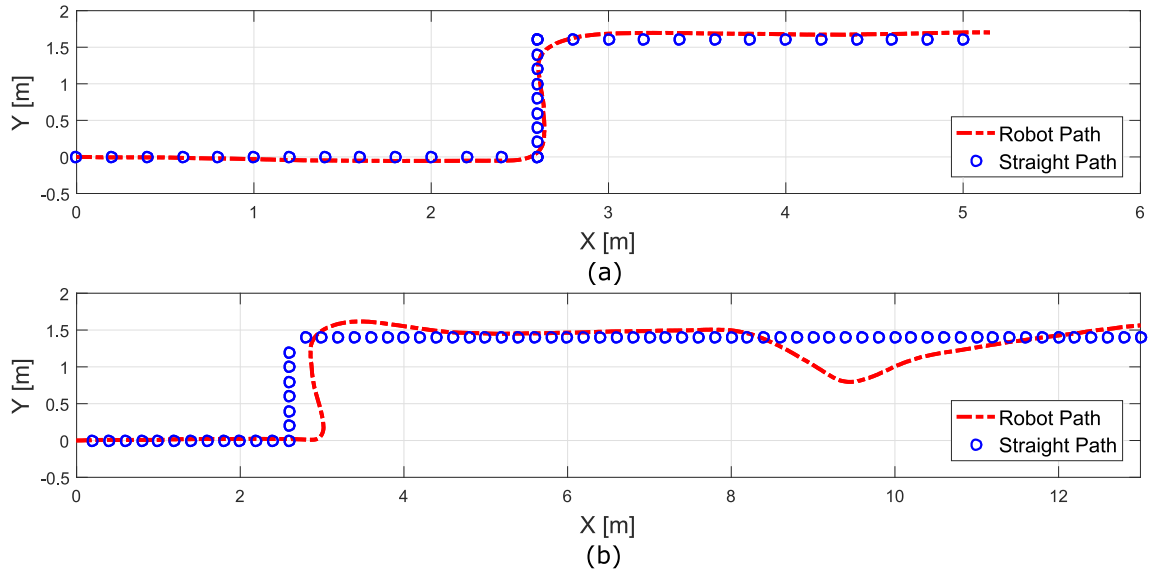

Fig. 12 Following the straight path. **a** Path following considering cognitive interface information. **b** Path following with induced error

interaction forces between the user and the walker increased while the user attempted to keep going forward (see Fig. 13). Once the user started to feel the controller action, the user was asked to follow the visual recommendation of the LEDs and to do a turn movement to the correct orientation. After following the controller recommendations through the multimodal cognitive interface for a while, the user was once again asked to deviate from the

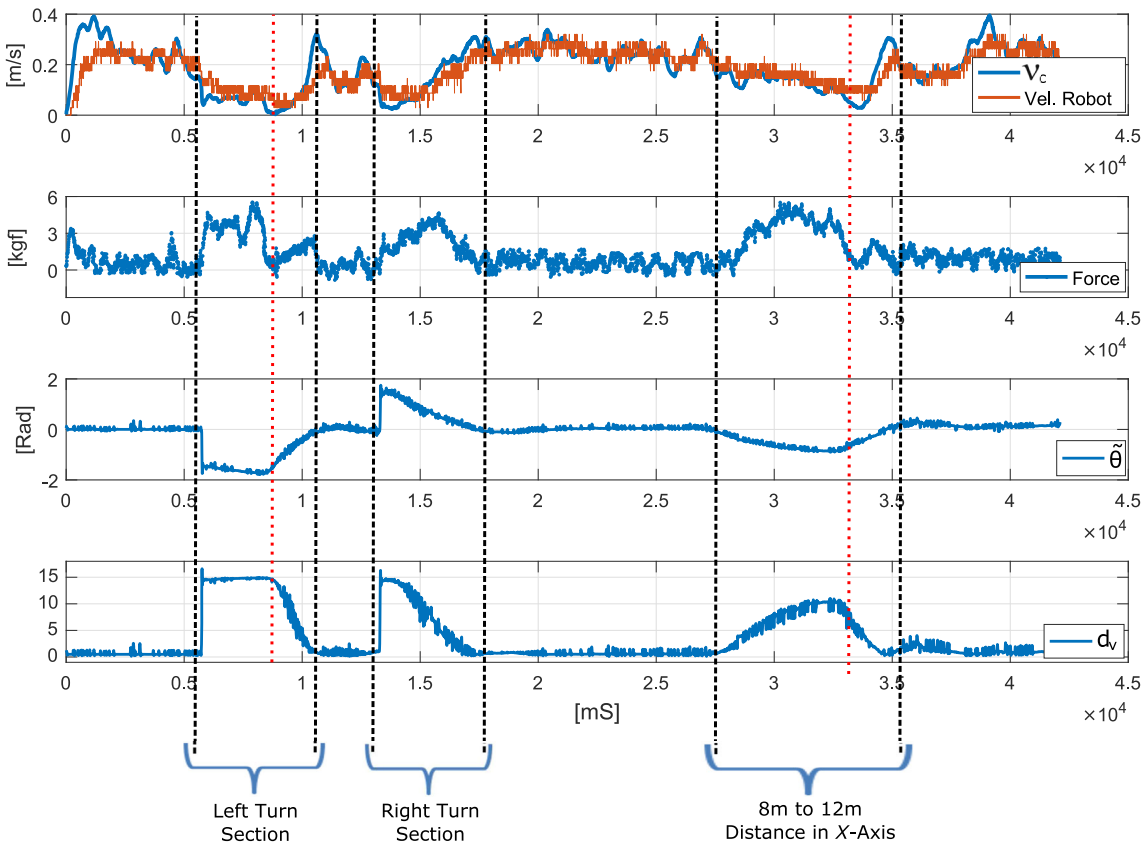

Fig. 13 Spatial modulation curve of d_v and haptic force response of the straight path of Fig. 12b. Up to down: Control and *SW* linear velocities, user's force signal, $\tilde{\theta}$ signal and d_v signal

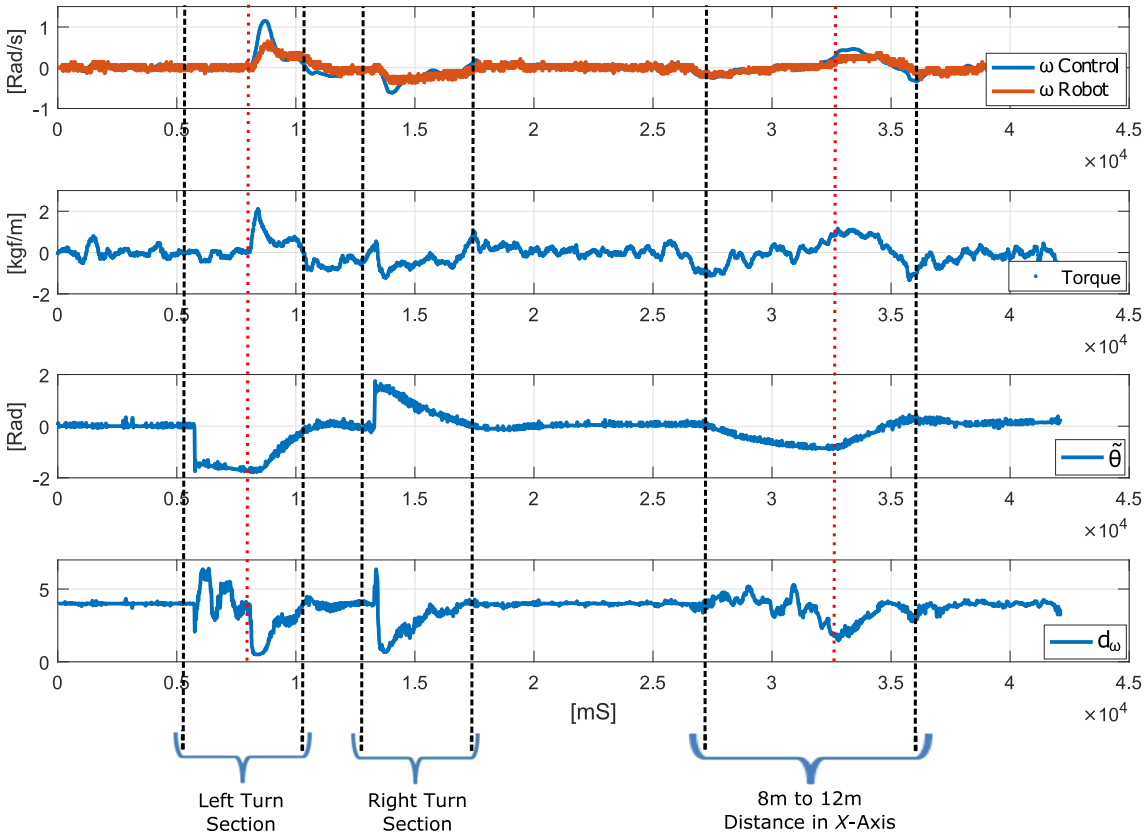

Fig. 14 Spatial modulation curve of d_ω and haptic torque response of the predetermined path in Fig. 12.b. Up to down: *SW* angular velocities, user's torque signal, $\tilde{\theta}$ and d_ω

predetermined path intentionally to force a reaction of the control strategy (see Fig. 12b at 8 m of distance in x axis approximately). Once the user could not keep going forward with the *SW*, the user was asked to follow the LEDs recommendations, rotating in the correct orientation and returning in the direction to the predetermined path.

A smaller guiding force is demanded to the user when the *SW* is on the predetermined path (see Fig. 13). In that situation, the parameter d_v assumes its minimum value, but, once d_v increases, it is observed that the user has to make more force to keep the locomotion (see black line spacing sections Fig. 13). While the walker is on the predetermined path, the force applied in the y axis of the sensors is between 0.2 kgf and 1 kgf, and the linear velocity of the device is higher (0.3 m/s approximately). When the spatial modulation acts, the linear velocity of the *SW* decreases to 0.05 m/s, and the user has to apply more force to move the *SW*. In this case, the *SW* is out of the predetermined path and the applied force is around or higher than 5 kg (see Fig. 13 -Force). At the strong changes of the predetermined path, i. e., on 90^o curves, the spatial modulator of d_v becomes saturated (see Fig. 13, left and right turn sections). The user interprets this as an uncomfortable effort that does not allow keeping going ahead. But, when the exit from the predetermined path is gradual, the user feels as the effort to move the SW goes increasing progressively. Thus, the user has to increase the force applied on the *SW* in order to move ahead (see Fig. 13, between 8 m and 12 m of distance in x axis section). In this case, the haptic feedback of the controller has a natural and intuitive interaction, generating a comfortable users' experience, as they do not make an effort to maneuvering the *SW*. Figure 14 shows the control signals related to the torque. In this case, when an error in $\tilde{\theta}$ is present, it can be observed that the signal of $d\omega$ begins to increase. The user feels the haptic feedback when doing a wrong orientation change on its own axis (see Fig. 14 -Torque). In this context, when the user rotates around its own axis with the intention of correcting the angular position error $\tilde{\theta}$, the torque needed to rotate decreases (see red dotted line on Figs. 13 and 14, at the left turn section). Therefore, the linear velocity of the *SW* begins to increase. Once it is found in the correct direction, it is not necessary to apply torque anymore, hence, the angular velocity decreases to 0 rad/s approximately. The section between 8 m to 12 m of distance in the x axis of Figs. 13 and 14, shows that the *SW* goes out from the predetermined path intentionally. It can be observed that when the user begins to rotate towards the predetermined path, the torque applied by the user to

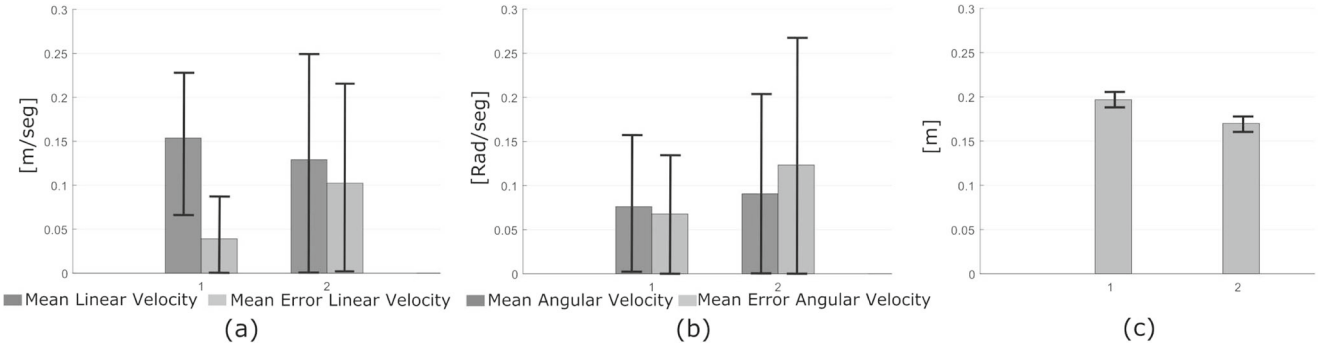

Fig. 15 Errors in the following of the straight path. Group 1: Second part of the experiment No.1 (user 7 of Table 1). Group 2: Average data of path following by user in the first part of the experiment No. 1. **a** Linear velocity. **b** Angular velocity. **c** Kinematic Estimation Error (*KTE*)

manipulate the *SW* begins to decrease. When the correct orientation is reached, the linear velocity increases and the angular velocity decreases to become 0 rad/s (see Fig. 14 -Torque).

Additionally, Fig. 14 shows that when the user applies a torque in a wrong direction (see Fig. 14), the value of the d_ω increases and the angular velocity of the *SW* decreases. This leads the user to apply more torque to keep rotating. Nevertheless, when the user wants to correct the angular position error $\tilde{\theta}$ or follow the visual cognitive interface, the value of $d\omega$ becomes minimum. In such case, the torque and $\tilde{\theta}$ have contrary signs. This is reflected to the user as a soft turn movement, easing the *SW* maneuverability. Through the signals of Figs. 13 and 14, it can be observed the feedback form that the admittance spatial modulation controller has on the user. This haptic feedback becomes a signal for the *HREI* and, consequently, a natural and intuitive way to guide the user on a predetermined path. At the experiment No. 1, the absolute error of linear and angular velocities of the controller was analyzed, and so the velocities. The *Kinematic Estimation Error (KTE)*, shown in Eq. 11 [27], compared the path traveled to the predetermined path:

$$KTE = \sqrt{|\overline{\varepsilon}|^2 + \sigma^2}, \tag{11}$$

where $|\overline{\varepsilon}|^2$ is the mean square of the errors between the predetermined path and the path followed by the *SW*, and σ^2 is the variance of this data. Thus, KTE also increases with the increase of variance.

In Fig. 15, the bars of Group No. 1 refer to the data collected from the user 7 (see Table 1) in the second part of the experiment No. 1. The travel along the predetermined path shown in Fig. 12b is also performed by user 7. The data that correspond to the Group No. 2 are referred to the 8 users of the experiment. In addition, it can be observed that the linear velocity error oscillates between 0.12 m/s and 0.15 m/s (see Fig. 15a), and the angular velocity error oscillates between 0.075 rad/s and 0.08 rad/s (see Fig. 15b). This is because no participant had any training with the *SW*, and hence some of them were cautious at the moment of manipulating the walker. For some users, it was not easy to keep the motion close to the predetermined path, because they did not know the path and could not see it. Therefore, they had to apply torques mainly guided by the LEDs. This is evidenced in the absolute error average calculated for the angular velocity (see Fig. 15). Regarding the path following, it is shown that the user 7 had a higher *KTE* error, because this user was intentionally asked to induce errors during the travel along the predetermined path on the second part of the experiment. Nevertheless, the *KTE* with variance ± 0.019 to Group 1 and ± 0.017 to Group 2 never went over 0.2 m in both cases (see Fig. 15c), which seems to be adequate to comply the purpose of guiding the user.

4.2 Experiment No. 2: Finding the Circle Path

In relation to experiment No. 2, once the users learned how to handle the *SW*, this experiment was aimed at finding the predetermined path, whose start point was away from him/her. Here, the users were guided by the multimodal cognitive interaction, and by physical interface through the haptic feedback. Two representative result can be observed in Fig. 16. Figure 16a shows how the user was guided by the haptic feedback until finding the circle, and Fig. 16b shows how the user was able to find the path aided by the multimodal cognitive interaction. When the haptic feedback is used, the path followed by the user presents oscillations, due to the virtual limits of the canal for easier locomotion defined by d_v and d_ω through the spatial modulation. Once this limits are overpassed, the controller begins to change dv and d_ω, and the user begins to feel the difficulty for locomotion, establishing the zone where he/she can move.

If the visual interface is used, the *SW*'s handling becomes softer and, consequently, it is easier to maintain on the predetermined path, once this is found (see Fig. 16a). When

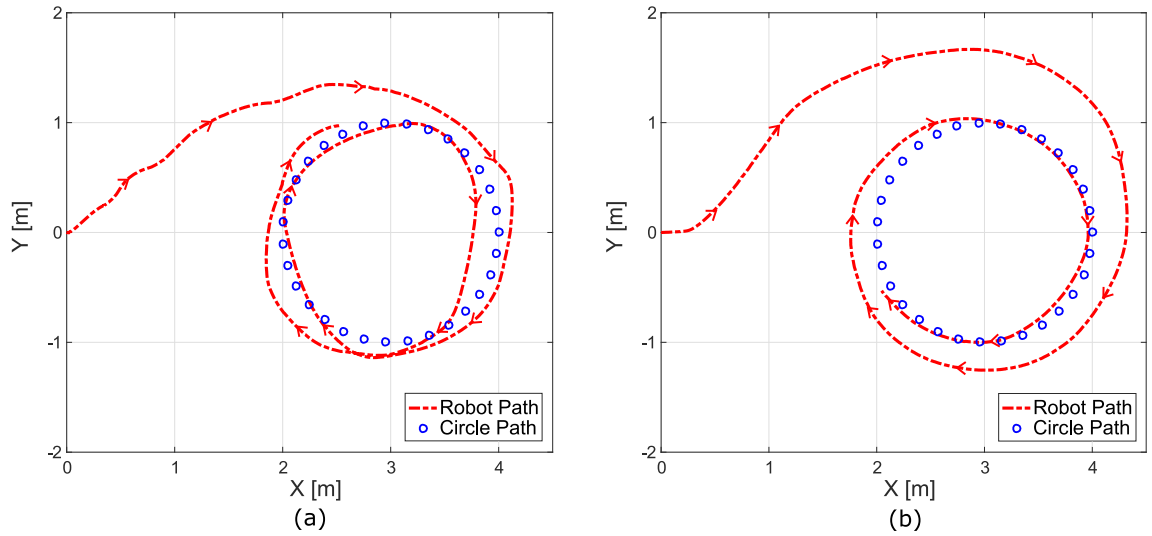

Fig. 16 Finding the circle path. **a** Finding the path with the haptic feedback. **b** Finding the path with the multimodal cognitive interaction

the movement is based on the LEDs recommendation and the haptic feedback, the virtual limits of the channel, for easier locomotion, are determined a little bit after the LEDs begin to turn on in an intermittent way. This way, the user knows that he/she has to do a soft turn in the direction provided by the LEDs, either right or left. On the contrary, if the LED is on always, but, not in an intermittent way, the mobility with the *SW* is the hardest, as a consequence of the admittance spatial modulation strategy. Also, it is observed that the user takes more time to find the circle path when using the multimodal cognitive interaction because he/she needs to process more information. The LEDs signals and haptic feedback together imply a more complex cognitive process. Such process introduces natural delays due to the information processing by the user[19]. However, the path travel time may be reduced by training with the SW. The effect of such training process is an ongoing study. Figure 17 shows the statistic error calculated once the *SW* is on the predetermined path. When the haptic feedback is used, the maximum position error is 0.3 m, once the user is on the path (as shown in Fig. 16b). The position error value is due to the hard torque movement that has to do the user to correct the *SW* direction. This error can decrease once the user has more training with the handling of the *SW*, or by doing an adjustment of the virtual masses assigned for m_v and m_ω (see Table 1), because depending on these values, the *SW* maneuverability becomes easier or harder. The *KTE* calculated when the user is guided through the multimodal cognitive interaction is 0.1617 $\pm$0.0295 m (see Fig. 17). This value is lower compared with the following error when the person is guided by the haptic feedback (0.3 $\pm$0.1337 m).

The user does not keep all the time on the predetermined path when using only the haptic feedback, as a consequence of the movement within the limits established by the virtual mobility canal for easier locomotion. Furthermore, with this experiment, it is verified that the two channels of the multimodal cognitive interaction are complementary when guiding the user along the predetermined path. The control strategy proposed in this work, makes the user feel comfortable when him/her is maneuvering the SW. The user has enough freedom in controlling the assistance robot movement, within limits established by the spatial admittance modulator.

To evaluate the acceptance of the proposed control strategy, qualitative questionnaires were applied after the participants had finished the two experiments. Figure 18 shows the results of two main questions, which report the perception of the participants about the control strategy. In general, the participants accepted the proposed control

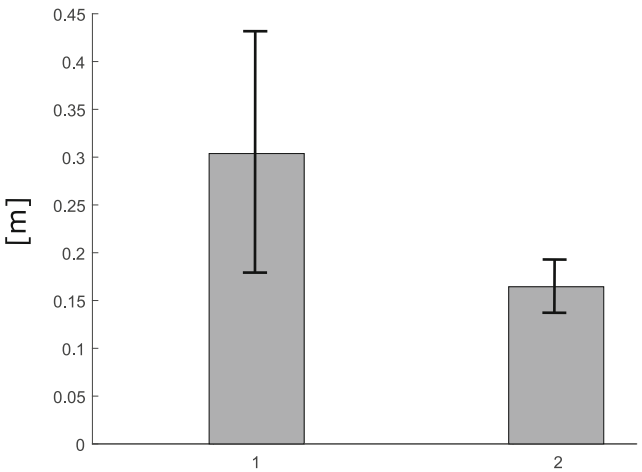

Fig. 17 Kinematic estimation error (*KTE*). Group 1: with haptic feedback. Group 2: with multimodal cognitive interaction

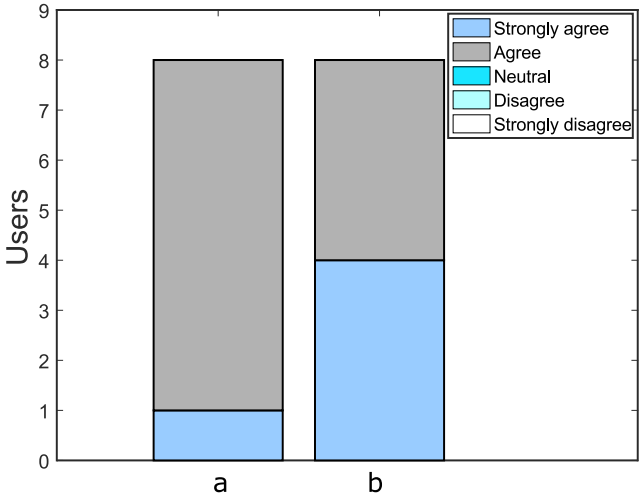

Fig. 18 Qualitative evaluation for the guided experiments. Questions: **a** "I felt that the SW was guiding me"; **b** "I felt an intuitive interaction with the smart walker"

strategy and the multimodal cognitive interaction. Although the average ratings were relatively high, Fig. 18a shows a trouble related to the way of guiding the user. We believe that the width of $d_v(t)$ function influenced the results. Hence, the virtual limits of the canal for easier locomotion may be lower. Once determined the mass values, the participants agreed that the handling of the SW was intuitive (see Fig. 18b). Also, comments on "safe-driving the SW", "ease of control", "natural interaction", "good velocity of locomotion" and "ease of learning", were registered after the experiments.

4.3 Experiment No. 3: Checking the Supervisor Functionality

Regarding the supervisor functionality, its performance was verified in two different experiments. In the first one, the predetermined path of experiment No. 1 (see Fig. 12b) was used to validate the visual interface. In the second experiment a straight line is used as predetermined path to verify the two safety factors established for the controller supervisor. The initial position was at $x = 0$ and $y = 0$. During this straight path, a bad position of the user in the *SW* was simulated through the force sensors. Furthermore, the supervisor answer was checked when the sensor RP-LIDAR detected an obstacle within the protection zone (see Fig. 9). Figure 19 shows the LEDs activation every time that an error in $\tilde{\theta}$ higher than ± 0.43 *Rad* or $\pm 25^0$ occurs. According to the predetermined path of Fig. 12b, the LEDs recommended a turn in the direction to correct the angular position error $\tilde{\theta}$ (see dashed line section zones of Fig. 19). This way, it is easier to the user interpret the turn direction that he/she must undertake in order to correct the orientation error and, consequently, to get into the zone where the *SW* is easier to maneuver .

The performance of the safety supervisor parameters is shown in Fig. 20. The different situations where the linear and angular velocities of the *SW* become zero are represented in the framed zones through red segmented lines. In zone (1), it can be observed that the controller detects the force signal as an indicator of starting the mobility, however, the supervisor does not detect force on the z axis in each sensor, therefore, the velocities of *SW*

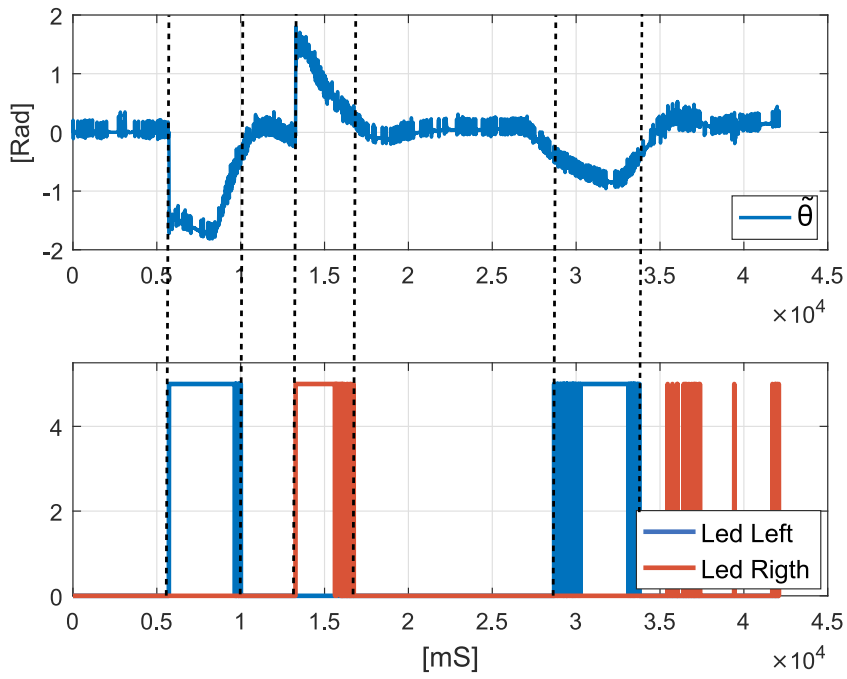

Fig. 19 Recommendation of turn by cognitive interface signals

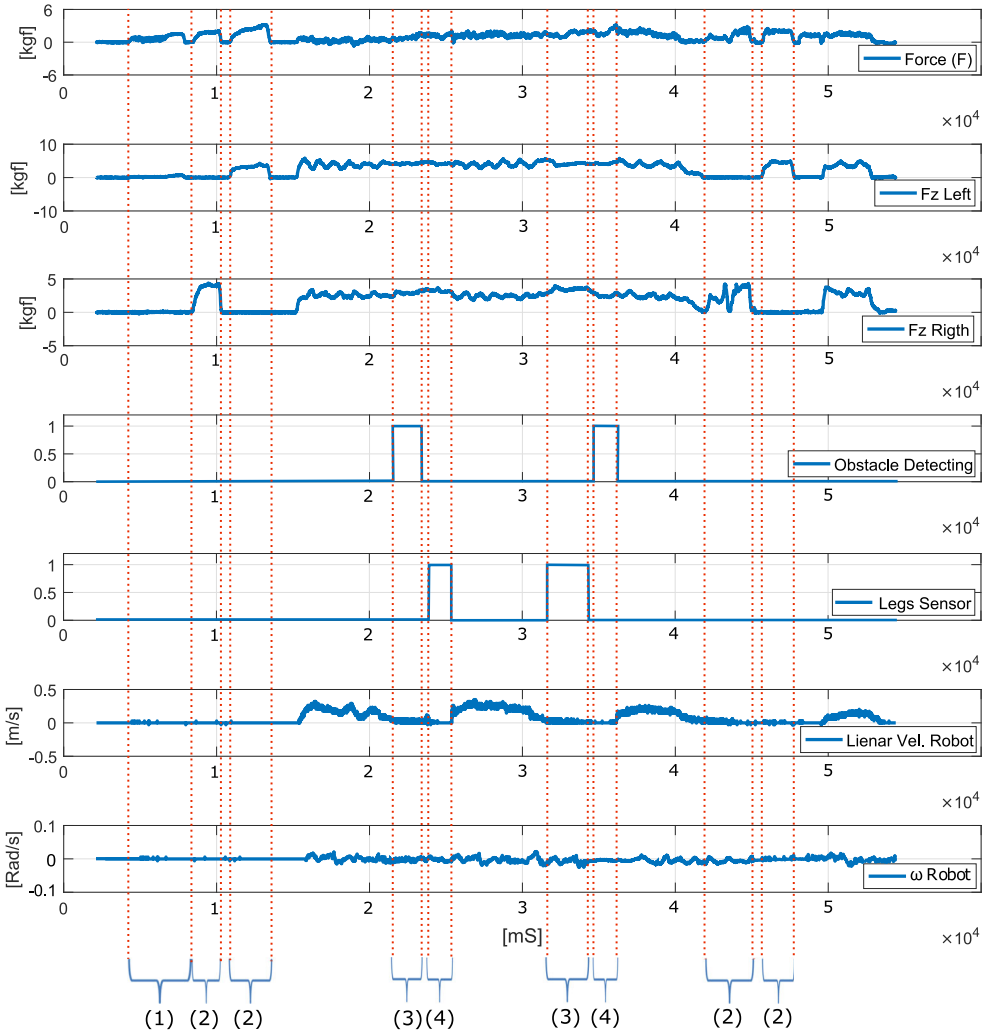

Fig. 20 Safety parameters of supervisor

become zero. In zone (2), a bad user's position on the *SW* is simulated, showing that the velocities continue being zero, as long as the supervisor does not detect the signal of z axis in both sensors. In zone (3), the RP-LIDAR sensor detects an object that enters into the protected region defined in front of the *SW*, and generates a flag for the supervisor. Then, the linear and angular velocities of the *SW* become zero and the collision is avoided. Once there is no obstacle anymore, the *SW* can take the velocity values provided by the control strategy. In zone (4), the LRF sensor detects that the distances established for this safety rule were exceeded, generating a flag for the supervisor. Then, the linear and angular velocities of the SW become zero. This way, the risk of falls or collisions between the user and the SW are avoided. Moreover, it is evidenced that when the supervisor detects a force in the z axis of both sensors that surpasses the threshold established, and the controller has a force signal as a command of mobility, the *SW* achieves the velocities calculated by the proposed control strategy.

The controller proposed here not only can assist people with gait disabilities, but also assist blind people [7]. This is another interesting topic of research around the *SWs* with this spatial modulation controller.

5 Conclusions and Future Work

This paper presented a new proposal that contributes for a natural interaction between *Human–Robot–Environment* using a new criterion for admittance control, as it takes advantage of the generation of a haptic feedback while the user navigates with a SW. Complemented with the visual interface, the multimodal cognitive interaction here presented, makes more intuitive for the user the way to know which is the correct path by where he/she should make locomotion. On the other hand, the spatial modulation concept allows to establish virtual limits for an easier locomotion zone with the *SW*. This contributes in a positive way for the cognitive system of the user, as it promotes the

interaction between the user and the environment through the user's decisions.

One of the advantages of this controller is the use of only one sensor to define the natural interaction *Human–Robot–Environment*, which is reflected in the computational efficiency and in the processing of control algorithm in real time. In this case, the experimental study allowed obtaining optimal results in terms of performance, at the moment of following or finding a predetermined path for the locomotion with the walker. This was verified through real experiments where the user, by means of the control strategy, could maintain himself/herself within the path using the controller recommendations through multimodal cognitive interaction.

The use of a haptic feedback as resulted from the physical interaction between user an *SW* contribute to a research area of interest for assistance tools for people's mobility. Through a sensation that is not visual or auditive, the user of the *SW* can obtain information that is related to his/her environment, thanks to the physical interaction of the arms with the *SW*.

As future work, we are developing new control strategies that promote the haptic feedback for the user of the *SWs*. Besides, with the RP-LIDAR sensor, the aim is to have more information about the environment to be used in probabilistic techniques such as SLAM to define the path that the *SW* should follow to reach an objective point. Additionally, it is necessary to introduce algorithms of obstacle avoidance to complete the navigation system of the UFES's *SW*. A new study was started to allow defining a selection model for the values of the virtual masses m_v and m_ω, and, in this way, to optimize the controller haptic feedback on the user.

Acknowledgements This research is supported by CAPES [grant number 88887.095626/2015-01], FAPES [grant number 72982608] and CNPq [grant number 304192/2016-3]. It is also acknowledged the support given by the National University of San Juan, Argentina.

References

1. Population Division United Nations, Department of Economic and Social Affairs: World Population Ageing 2015 Technical report (2015)
2. Alexander, N.B., disorders, A.G.: Gait search for multiple causes. Cleveland Clinic J. Med. **72**(7), 586–600 (2005)
3. Shields, M.: Use of wheelchairs and other mobility support devices **15**(3), 37–41 (2014)
4. Bradley, S.M., Hernandez, C.R.: Geriatric assistive devices. Am. Fam. Phys. **84**(4), 405–411 (2011)
5. Bateni, H., Maki, B.E.: Assistive devices for balance and mobility: Benefits, demands, and adverse consequences. Arch. Phys. Med. Rehab. **86**, 134–145 (2005)
6. Martins, M.M., Santos, C.P., Frizera-neto, A., Ceres, R.: Assistive mobility devices focusing on smart walkers classification and review. Robot. Auton. Syst. **60**(4), 548–562 (2011)
7. Wachaja, A., Agarwal, P., Zink, M., Reyes, M., Mòller, K., Burgard, W.: Navigating blind people with walking impairments using a smart walker. Auton. Robot., 1–19 (2016)
8. Morone, G., Annicchiarico, R., Iosa, M., Federici, A., Paolucci, S., Cortès, U., Caltagirone, C.: Overground walking training with the i -Walker, a robotic servo-assistive device, enhances balance in patients with subacute stroke: A randomized controlled trial. J. Neuro Eng. Rehab. **13**, 1–10 (2016)
9. Mf, C., Mou, W., Liao, C.K., Fu, L.C.: Design and implementation of an active robotic walker for Parkinson's patients. SICE Annual Conference, pp. 2068–2073 (2012)
10. Cifuentes, C.A., Frizera, A.: Human-Robot Interaction Strategies for Locomotion. Springer International Publishing, Switzerland (2016)
11. Robinson, H., MacDonald, B., Broadbent, E.: The role of healthcare robots for older people at home: A review. Int. J. Soc. Robot. **6**(4), 575–591 (2014)
12. Martins, M., Santos, C., Frizera, A., Ceres, R.: A review of the functionalities of smart walkers. Med. Eng. Phys. **37**(10), 917–928 (2015)
13. Lacey, G.J., Rodriguez-losada, D.: The evolution of Guido. IEEE Robot. Autom. Mag. **15**, 75–83 (2008)
14. Lee, G., Ohnuma, T., Young, N.: Design and control of JAIST active robotic walker. Intell. Serv. Robot. **3**, 125–135 (2010)
15. Valadão, C., Caldeira, E., Bastos-Filho, T., Frizera-Neto, A., Carelli, R.: A new controller for a smart walker based on human-robot formation. Sensors (Switzerland) **16**(7), 1–26 (2016)
16. Geravand, M., Werner, C., Hauer, K., Peer, A.: An integrated decision making approach for adaptive shared control of mobility assistance robots. Int. J. Soc. Robot. **8**(5), 631–648 (2016)
17. Haoyong, Y., Spenko, M., Dubowsky, S.: An adaptive shared control system for an intelligent mobility aid for the elderly. Auton. Robot. **15**, 53–66 (2003)
18. Reyes Adame, M., Yu, J., Moeller, K.: Mobility support system for elderly blind people with a smart walker and a tactile map. In: XIV Mediterranean conference on medical and biological engineering and computing, vol. 57, pp. 602–607. Springer, Cham (2016)
19. José, L.: (CSIC) Pons. Wearable Robots: Biomechatronic Exoskeletons. Wiley, Madrid (2008)
20. Rampeltshammer, W., Peer, A.: Control of mobility assistive robot for human fall prevention. In: 2015 IEEE International Conference on Rehabilitation Robotics (ICORR), pp. 882–887. IEEE Xplore (2015)
21. Ko, C.H., Young, K.Y., Yi, C.H., Agrawal, S.K.: Active and passive control of walk-assist robot for outdoor guidance. IEEE/ASME Trans. Mechatron. **18**(3), 1211–1220 (2013)
22. Cheng-kai, L., Huang, Y.-c., Lee, C.-j.: Adaptive guidance system design for the assistive robotic walker. Neurocomputing **170**, 152–160 (2015)
23. Cortès, U., Martinez-velasco, A., Barrué, C., Benedico, T., Caltagirone, C., Annicchiarico, R.: A SHARE-it service to elders ' mobility using the i-Walker. Gerontechnology **7**, 95–100 (2008)
24. Egelman, D.M., Person, C., Montague, P.R.: A computational role for dopamine delivery in human decision-making. J. Cogn. Neurosci. **10**, 623–630 (1998)
25. Andaluz, V.H., Roberti, F., Toibero, J.M., Carelli, R., Wagner, B.: Adaptive dynamic path following control of an unicycle like mobile robot. In: Intelligent Robotics and Applications, chapter 56, pp. 563–574. Springer, Berlin (2011)

26. De la Cruz, C., Carelli, R.: Dynamic modeling and centralized formation control of mobile robots. In: IECON 2006 - 32nd Annual Conference on IEEE Industrial Electronics, pp. 3880–3885 (2006)
27. Neto, A.F., Gallego, J.A., Rocon, E., Pons, J., Ceres, R.: Extraction of user ' s navigation commands from upper body force interaction in walker assisted gait. Biomed. Eng. Online **9**(1), 1–17 (2010)

Mario F. Jiménez received the B.S. degree in Electronics Engineering from the Universidad de Ibagué, Ibagué, Colombia, in 2005 and the Industrial Control Engineering Master degree from the Universidad de Ibagué, Ibagué, Colombia, in 2012. He is currently working toward the Ph.D. degree in the Assistive Technology Group, Federal University of Espirito Santo, Vitória, Brazil. His current research interests include Human-Robot-Environment interaction and rehabilitation robotics.

Matias Monllor received the B.S. degree in Electronics Engineering from the Facultad de Ingenieria - UNSJ, San Juan - Argentina, in 2014. He is currently a Ph.D. student in Instituto de Automática, UNSJ - CONICET His current research interests include human–robot interaction and control.

Anselmo Frizeira received the B.S. degree in Electrical Engineering from the Federal University of Espirito Santo (UFES), Vitória, Brazil, in 2006 and the Ph.D. in Electronics from the Universidad de Alcalá, Alcalá, Spain, in 2010. From 2006 to 2010, he was a Researcher with the Bioengineering Group, Spanish National Research Council (CSIC). He is currently a Professor in the Department of Electrical Engineering, UFES. His research interests include rehabilitation robotics, human–machine interaction, and movement.

Teodiano Bastos received the B.S. degree in Electrical Engineering from the Universidade Federal do Espirito Santo, Vitória, Brazil, in 1987; the Specialization in Automation from the Instituto de Automatica Industrial, Madrid, Spain, in 1989; and the Ph.D. degree in Physical Science (Electricity and Electronics) from the Universidad Complutense de Madrid, Madrid, Spain, in 1994. He is currently a full Professor with the Universidade Federal do Espirito Santo, teaching and doing research at the Postgraduate Program in Electrical Engineering, the Postgraduate Program in Biotechnology, and the Northwest Network of Biotechnology Ph.D. Program. His current research interests include signal processing, rehabilitation robotics, and assistive technology for people with disabilities.

Flabio Roberti was born in Buenos Aires, Argentina. He graduated in Electronic Engineering from the National University of San Juan, Argentina in 2003; on March 2009 he obtained the Ph.D. degree in Control Systems Engineering at the Instituto de Automática, National University of San Juan. He is currently Professor at the National University of San Juan and Researcher of the National Council for Scientific and Technical Research (CONICET).

Ricardo Carelli was born in San Juan, Argentina. He received the B.S. degree in engineering from the National University of San Juan, San Juan, Argentina, and the Ph.D. degree in electrical engineering from the National University of Mexico, Mexico City, Mexico. He is a Full Professor at the National University of San Juan, where he is the Director of the Instituto de Automática. He is also a Senior Researcher with the National Council for Scientific and Technical Research (CONICET), Buenos Aires, Argentina. His research interests include robotics, manufacturing systems, adaptive control, and artificial intelligence applied to the automatic control. Prof. Carelli is a member of the Argentine Association of Automatic Control (AADECA-IFAC).